

Consistent closure modeling in large eddy simulations by direct approximation of the filtered advection term

Max Hausmann[†], Berend van Wachem

Chair of Mechanical Process Engineering, Otto-von-Guericke-Universität Magdeburg,
Universitätsplatz 2, 39106 Magdeburg, Germany

This article addresses the widely overlooked conceptual inconsistency of the large eddy simulation (LES) framework, namely that the commonly used advection term introduces higher wave numbers in the filtered Navier-Stokes equations than consistent with the definition of a filtered equation. It is explained how this inconsistency is the reason that flux limiters, stabilization terms, or dealiasing is often required and that the LES solution is typically mesh dependent. A consistent alternative is the direct approximation of the filtered advection term, for which we derive an exact expression based on an infinite series expansion with terms of increasing order in the filter width. We show that truncating the series expansion after few terms gives an expression that is highly correlated with the filtered advection term and a suitable LES model. A posteriori studies with decaying turbulence and a turbulent shear flow are conducted that reveal that the proposed approximation of the filtered advection term predicts improved kinetic energy spectra and filtered velocity correlations compared to classical LES.

Key words: large eddy simulation; turbulence modeling; subgrid-scale modelling

1. Introduction

Many attempts have been made in the past decades to address the long standing problem of reliable long term predictions of turbulent flows. One of the most promising approaches is the solution for the spatially low-pass filtered flow field, which is commonly known under the name large eddy simulations (LES). Modern applications of LES show surprisingly few differences in their methodology compared to the pioneering works of Smagorinsky (1963), Lilly (1966), Deardorff (1970), and Leonard (1975).

The central modeling challenge in LES consists of finding an expression for the filtered advection term, $\overline{u_i u_j}$, that contains only known filtered quantities, such as the filtered velocity $\overline{u_i}$. With very few exceptions, the filtered advection term is nowadays still approximated as $\overline{u_i u_j} = \overline{u_i} \overline{u_j} + \tau_{ij}$, where τ_{ij} are the modeled subfilter stresses, similar to the early LES studies mentioned above. There are good reasons for choosing this approximation of the filtered advection term. The dyadic product of the filtered velocities, $\overline{u_i} \overline{u_j}$, can be shown to be the lowest order approximation of $\overline{u_i u_j}$ (see, e.g., Vreman *et al.* (1996); Leonard (1997))) and constitutes a convenient choice in numerical simulations because the advection term is identical to the advection term in the Navier-Stokes equations (NSE) if the flow quantities are interpreted as being filtered. However, $\overline{u_i u_j}$

[†] Email address for correspondence: max.hausmann@ovgu.de

and $\bar{u}_i\bar{u}_j$ differ in a fundamental property that has severe consequences in practical applications of LES, that is, the range of wave numbers that both terms span. While $\overline{u_i u_j}$ is bandwidth limited at the maximum wave number of the filtering operation, $\bar{u}_i\bar{u}_j$ generally contains higher wave numbers. Therefore, it is not sufficient if the LES resolution is fine enough to resolve the filtered velocity because the high wave numbers of $\bar{u}_i\bar{u}_j$ remain unresolved. In practice, flux limiters, stabilization terms, or dealiasing are introduced to dampen the contribution of the unresolved wave numbers of $\bar{u}_i\bar{u}_j$. The discretization errors can be of the same order or even greater than the subfilter stress contribution itself (Ghosal 1996). This means that the flow solution strongly depends on the numerical discretization and that the fundamental principle in computational fluid mechanics is violated, namely that the solution should converge as the mesh is refined. A whole branch of LES, the so-called implicit LES, rely exclusively on a manufactured discretization error without any explicit closure modeling (Margolin *et al.* 2006; Grinstein *et al.* 2007). However, the lack of a definition of a filter kernel in implicit LES renders a rigorous validation of the results with explicitly filtered DNS (FDNS) results impossible. When the filter kernel is clearly defined and the non-linear interactions between the filtered and subfilter scales are explicitly accounted for by a modeled term, the LES is called explicit (Sagaut 2005). It is possible to derive an exact infinite series expansion for these non-linear interactions for filter kernels that are commonly used (Vreman *et al.* 1996). Although the terms of the series expansion have increasing orders of the filter width suggesting that they become smaller, all terms are products of spatial derivatives of the filtered velocity, which contain high wave numbers that are not suitable for LES with a coarse resolution. Germano (1986) derived an exact expression for the filtered advection term based on elliptic differential filters that consists of a finite number of terms. Filtering with an elliptic differential filter is equivalent to convolution with a singular filter kernel that decays slowly in spectral space, which is not well suited to remove sufficient high wave number content to justify a coarse resolution. Another formally exact expression for the filtered advection term can be obtained by approximate deconvolution of filtered quantities (Stolz & Adams 1999; Stolz *et al.* 2001) resulting in an infinite series containing consecutively filtered quantities. Although approximate deconvolution can be conceptually suitable to approximate the filtered advection term because the approximations contains only filtered products, its convergence strongly depends on the filter kernel and the potentially large number of explicit filtering operations can add a significant computational overhead.

In contrast to implicit LES and LES with explicit modeling of the subfilter stress tensor, τ_{ij} , that rely on flux limiters or stabilization terms, the filtered advection term $\bar{u}_i\bar{u}_j$ can be modeled directly, making any stabilizing numerical interventions unnecessary. The direct approximation of the filtered advection term has been discussed in previous studies (Lund 2003; Bose *et al.* 2010; Singh *et al.* 2012). Lund (2003) makes the important point that the dyadic product of the filtered velocities used in classical LES, $\bar{u}_i\bar{u}_j$, introduces too large wave numbers. The models proposed in Lund (2003); Bose *et al.* (2010) rely on an advection term of the type $\overline{\bar{u}_i\bar{u}_j}$ supplemented with a dynamic Smagorinsky model (Germano *et al.* 1991; Lilly 1992) that, as demonstrated in section 3.2, is even less correlated with the filtered advection term than the dyadic product of the filtered velocities, $\bar{u}_i\bar{u}_j$, used in classical LES. The models proposed in Singh *et al.* (2012) contain products of filtered quantities and, therefore, introduce high wave numbers in the filtered NSE, similar to the classical advection term relying on the dyadic product of the filtered velocities.

In the present article, an expression for the filtered advection term is derived that is an infinite series expansion in powers of the filter width, which is exact and contains only

terms that are filtered. Therefore, the proposed approximation for the filtered advection term only contains wave numbers consistent with the definition of a filtered quantity. It is shown that truncating the series expansion for the filtered advection term after few terms allows for an approximation of the filtered advection term that is highly correlated with the actual filtered advection term. Furthermore, it is shown that the expression predicts the total energy transfer associated to the filtered advection term and its spectral distribution increasingly accurate with increasing order. The proposed expression does not require any flux limiters, stabilization terms, or dealiasing, converges under mesh refinement, and is shown to predict more accurate flow statistics in decaying turbulence and a turbulent shear flow than classical LES.

The remainder of this article is structured as follows. The common practice and the limitations of classical LES are discussed in section 2. In section 3, the exact expression for the filtered advection term is derived and investigated in homogeneous isotropic turbulence (HIT). The results of two validation cases are shown and discussed in section 4 and guidelines for the implementation of the proposed modeling are provided in section 5 before the article concludes with section 6.

2. Classical LES formulation

2.1. Filtered Navier-Stokes equations

It is assumed that the flow quantities are defined in an unconfined or infinite domain, Ω_f . To remove the high wave number content of a generic flow quantity, Φ , a spatial low pass filter is applied to Φ that is defined as

$$\bar{\Phi}(\mathbf{x}, t) = \int_{\Omega_f} g(\mathbf{x} - \mathbf{y})\Phi(\mathbf{y}, t)dV_y, \quad (2.1)$$

where $\bar{\Phi}$ is the filtered flow quantity. The filter kernel, g , is assumed to be symmetric, spatially uniform, and satisfies

$$\int_{\Omega_\infty} g(\mathbf{x})dV_x = 1, \quad (2.2)$$

where Ω_∞ represents an infinite domain. Since spatially uniform filter kernels commute with spatial derivatives and filter kernels that are constant in time commute with temporal derivatives, the filtered NSE of a flow with constant density, ρ_f , and constant dynamic viscosity, μ_f , are given as

$$\frac{\partial \bar{u}_i}{\partial x_i} = 0, \quad (2.3)$$

$$\rho_f \frac{\partial \bar{u}_i}{\partial t} + \rho_f \frac{\partial \bar{u}_i \bar{u}_j}{\partial x_j} = -\frac{\partial \bar{p}}{\partial x_i} + \mu_f \frac{\partial^2 \bar{u}_i}{\partial x_j \partial x_j}, \quad (2.4)$$

where \bar{u}_i is the filtered velocity and \bar{p} is the filtered pressure. If the filter kernel g is zero beyond a wave number k_c , every term in equation (2.3) and equation (2.4) is also zero at wave numbers larger than k_c . Therefore, if the numerical resolution is high enough to represent functions with the wave number k_c , it is also sufficient to resolve every term of the filtered NSE.

The filtered NSE as given in equations (2.3)-(2.4) are exact since no additional modeling assumptions are introduced on top of the validity of the NSE.

2.2. Classical LES decomposition

The fundamental problem of the filtered momentum equation (2.4) is that the filtered advection term is not closed, i.e., it requires knowledge of the unfiltered velocity to be computed. Therefore, in what we refer to as classical LES, the filtered advection term is approximated as

$$\overline{u_i u_j} = \overline{u_i} \overline{u_j} + \tau_{ij}, \quad (2.5)$$

where τ_{ij} is the subfilter stress tensor that requires modeling. It can be shown by Taylor series expansion of the filtered velocity that $\overline{u_i} \overline{u_j}$ is the lowest order approximation of $\overline{u_i u_j}$ (see, e.g., Vreman *et al.* (1996); Leonard (1997)). Furthermore, the decomposition (2.5) satisfies Galilean invariance exactly if τ_{ij} is Galilean invariant and the filtered NSE can be solved with a standard flow solver, as it used for DNS, by just adding an additional momentum source representing the modeled contribution of τ_{ij} .

2.3. Limitations of classical LES formulations

The major limitation of employing the classical LES decomposition given in equation (2.5) is that $\overline{u_i} \overline{u_j}$ and τ_{ij} both contain nonzero amplitudes of wave numbers larger than k_c . As a consequence, $\overline{u_i} \overline{u_j}$ and τ_{ij} require a finer resolution to be represented accurately than $\overline{u_i}$. The reason is that any product of two functions that contain wave numbers up to k_c , generally contains wave numbers up to $2k_c$. A simple example of this property is, for instance, the square of a sine-function, which gives $\sin(k_c x) \sin(k_c x) = \frac{1}{2}(1 - \cos(2k_c x))$. After applying the Fourier transform to the filtered NSE that contain the classical LES decomposition given in equation (2.5), it can be observed that there are only two nonzero terms remaining in the wave number range $k \in (k_c, 2k_c)$ and the Fourier transformed filtered NSE reduce to

$$\mathcal{F}\{\overline{u_i} \overline{u_j}\}(\mathbf{k}) + \mathcal{F}\{\tau_{ij}\}(\mathbf{k}) = 0, \quad |\mathbf{k}| \in (k_c, 2k_c), \quad (2.6)$$

where \mathcal{F} indicates the Fourier transform. All other terms in the filtered momentum equation are filtered and are zero at wave numbers larger than k_c . This is illustrated in figure 1, where the filtered and unfiltered kinetic energy spectrum are shown together with the wave number range in which equation (2.6) holds. The filtered NSE with the classical LES decomposition of the advection term is still exact if the model for τ_{ij} is exact. Since the model for τ_{ij} generally contains a modeling error, equation (2.6) is not exactly satisfied, which results in a predicted velocity that is nonzero when solving the filtered NSE, even at wave numbers larger than k_c . Thus, the predicted field of $\overline{u_i} \overline{u_j}$ contains wave numbers that even exceed $2k_c$, which means that there is a successive propagation of the modeling error towards smaller scales. This not only violates the definition of the filtered velocity that can contain only wave numbers up to k_c , but also requires a sufficiently high numerical resolution to represent the high wave number content sufficiently accurate.

In practice, the numerical resolution is typically chosen to be just fine enough to resolve wave numbers up to k_c . The larger wave numbers resulting from the inaccurate modeling of τ_{ij} cannot be resolved and appear as discretization error. Even if τ_{ij} is explicitly modeled, the solution strongly relies on the discretization error and therefore cannot be consistently classified as explicit LES in the classical sense.

In addition to the active wave number range, the decomposition of the filtered advection term also has an influence on the structural properties of the filtered flow field. The filtered flow structures are directly influenced by the model for τ_{ij} , but the vast majority of models is relying on the Boussinesq hypothesis, i.e., on a turbulent viscosity (Smagorin-

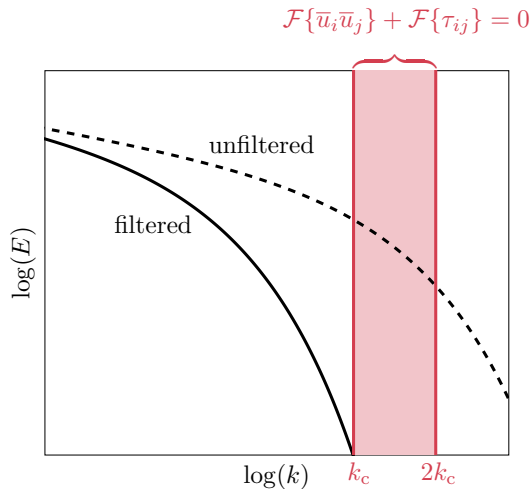


FIGURE 1. Sketch of the filtered and unfiltered kinetic energy spectrum, E , as a function of the wave number, k . With the classical decomposition of the advection term, the advection term and τ_{ij} are even nonzero in the highlighted wave number range that lies beyond the maximum wave number of the velocity field, k_c .

sky 1963; Germano *et al.* 1991; Nicoud & Ducros 1999; Vreman 2004). With a turbulent viscosity model, the filtered NSE only differ by a viscosity from the unfiltered NSE, which is why classical LES with a turbulent viscosity model closely resemble the flow structures of an unfiltered DNS at a smaller Reynolds number (Kamal & Johnson 2024; Arun *et al.* 2025). However, the flow structures of the explicitly FDNS differ significantly from the LES with a turbulent viscosity model. The LES produces elongated flow structures that span a wide wave number range in different directions, but the explicit FDNS velocity contains much more isotropic filtered flow structures, which is shown in section 4.1.2.

3. An expression for the filtered advection term

3.1. Derivation

To close the filtered NSE given in equations (2.3)-(2.4), an expression for the filtered advection term, $\bar{u}_i \bar{u}_j$, is required. As explained in the previous section, the expression for the filtered advection term should be bandwidth limited with the largest wave number being the cutoff wave number determined by the filter kernel in order to ensure that the filtered velocity also remains bandwidth limited in accordance to its definition when the filtered NSE are solved.

In the following, a Gaussian filter kernel with a standard deviation σ is assumed for the filter kernel g . One of the advantages of a Gaussian over other common filter kernels is that it rapidly decays in real and spectral space. A rapidly decaying kernel in real space allows for computationally feasible explicit filtering in LES and a kernel that is rapidly decaying in spectral space is required to remove high wave number content of the flow field to justify a coarse resolution in LES. According to the uncertainty principle (Stein 2003), a nonzero function cannot be compactly supported in real and in spectral space and a rapidly decaying kernel in real space leads to a slowly decaying kernel in spectral space and vice versa. The top-hat filter kernel commonly used in LES has compact support in real space but decays slowly in spectral space, which is why it is not well suited to represent the filtered solution with a coarse numerical resolution.

Although a Gaussian filter kernel does not have compact support in spectral space, it decays exponentially with increasing wave number. According to the definition of a bounded filtered quantity, the approximation for the filtered advection term should decay at least as rapidly as a Gaussian (times a real finite constant) for large wave numbers. An approximation of the filtered advection term violating this property can lead to a predicted “filtered” velocity that contains higher wave numbers than consistent with the definition of a filtered quantity as explained in section 2.3.

In the case of a Gaussian filter kernel, the filtering operation of a generic flow quantity, $\bar{\Phi}$, is equivalent to solving the following differential equation

$$\frac{\partial \bar{\Phi}(\mathbf{x}, t, \sigma)}{\partial(\sigma^2)} = \frac{1}{2} \frac{\partial^2 \bar{\Phi}(\mathbf{x}, t, \sigma)}{\partial x_k \partial x_k}, \quad \bar{\Phi}(\mathbf{x}, t, \sigma = 0) = \bar{\Phi}|_{\sigma=0} = \bar{\Phi}. \quad (3.1)$$

For conciseness, the dependencies space, time, and filter width will be dropped in the following.

Reformulating the convolution filtering given in equation (2.1) to the solution of a differential equation alone does not give a closed expression for the filtered advection term, because the formal solution of equation (3.1) requires knowledge of $\bar{\Phi}$ at smaller filter widths (Johnson 2020). Instead of considering the formal solution of equation (3.1), we proceed with the Taylor series expansion as a function of the squared filter width, σ^2 , given as

$$\bar{\Phi}|_{\sigma=0} = \bar{\Phi}|_{\sigma} - \sigma^2 \frac{\partial \bar{\Phi}}{\partial(\sigma^2)}|_{\sigma} + \frac{1}{2} \sigma^4 \frac{\partial^2 \bar{\Phi}}{\partial(\sigma^2)^2}|_{\sigma} - \frac{1}{6} \sigma^6 \frac{\partial^3 \bar{\Phi}}{\partial(\sigma^2)^3}|_{\sigma} + \mathcal{O}(\sigma^8). \quad (3.2)$$

This allows to express the flow quantity at a filter width equal to zero as a function of the filtered flow quantity and its derivatives with respect to σ^2 . To obtain an expression for the filtered advection term, a second generic flow quantity, $\bar{\Psi}$, is introduced that possesses an analog Taylor series. Computing the product $\bar{\Phi}|_{\sigma=0} \bar{\Psi}|_{\sigma=0}$ by multiplication of the respective Taylor series gives, after simplification,

$$\bar{\Phi}|_{\sigma=0} \bar{\Psi}|_{\sigma=0} = \bar{\Phi}|_{\sigma} \bar{\Psi}|_{\sigma} - \sigma^2 \frac{\partial \bar{\Phi} \bar{\Psi}}{\partial(\sigma^2)}|_{\sigma} + \frac{1}{2} \sigma^4 \frac{\partial^2 \bar{\Phi} \bar{\Psi}}{\partial(\sigma^2)^2}|_{\sigma} - \frac{1}{6} \sigma^6 \frac{\partial^3 \bar{\Phi} \bar{\Psi}}{\partial(\sigma^2)^3}|_{\sigma} + \mathcal{O}(\sigma^8). \quad (3.3)$$

By multiplying equation (3.1) with $\bar{\Psi}$, it can be shown that the second term of the Taylor series expansion can be expressed as a function of spatial derivatives of the filtered flow quantities

$$\frac{\partial \bar{\Phi} \bar{\Psi}}{\partial(\sigma^2)} = \frac{1}{2} \frac{\partial^2 \bar{\Phi} \bar{\Psi}}{\partial x_k \partial x_k} - \frac{\partial \bar{\Phi}}{\partial x_k} \frac{\partial \bar{\Psi}}{\partial x_k}. \quad (3.4)$$

Taking the derivative of the resulting term with respect to σ^2 gives an expression for the third term of the Taylor series expansion considering that filtering and spatial derivatives and spatial derivatives and derivatives with respect to σ^2 commute

$$\begin{aligned} \frac{\partial^2 \bar{\Phi} \bar{\Psi}}{\partial(\sigma^2)^2} &= \frac{\partial}{\partial(\sigma^2)} \left(\frac{1}{2} \frac{\partial^2 \bar{\Phi} \bar{\Psi}}{\partial x_k \partial x_k} - \frac{\partial \bar{\Phi}}{\partial x_k} \frac{\partial \bar{\Psi}}{\partial x_k} \right) \\ &= \frac{\partial^2}{\partial x_l \partial x_l} \left(\frac{1}{4} \frac{\partial^2 \bar{\Phi} \bar{\Psi}}{\partial x_k \partial x_k} - \frac{\partial \bar{\Phi}}{\partial x_k} \frac{\partial \bar{\Psi}}{\partial x_k} \right) + \frac{\partial^2 \bar{\Phi}}{\partial x_k \partial x_l} \frac{\partial^2 \bar{\Psi}}{\partial x_k \partial x_l}. \end{aligned} \quad (3.5)$$

Higher order terms of the Taylor series can be obtained analogously.

By replacing the generic flow quantities with the fluid velocity components, the filtered advection term $\bar{u}_i u_j = \bar{u}_i|_{\sigma=0} \bar{u}_j|_{\sigma=0}$ can be expressed as a function of the filtered velocity for any arbitrary order of the filter width. An approximation of the filtered advection

term up to the zero order term is given as

$$\overline{u_i u_j} = \overline{\bar{u}_i \bar{u}_j} + \mathcal{O}(\sigma^2), \quad (3.6)$$

up to the second order term as

$$\overline{u_i u_j} = \overline{\bar{u}_i \bar{u}_j} - \sigma^2 \left[\frac{1}{2} \frac{\partial^2 \bar{u}_i \bar{u}_j}{\partial x_k \partial x_k} - \frac{\partial \bar{u}_i}{\partial x_k} \frac{\partial \bar{u}_j}{\partial x_k} \right] + \mathcal{O}(\sigma^4), \quad (3.7)$$

and up to the fourth order term as

$$\begin{aligned} \overline{u_i u_j} = & \overline{\bar{u}_i \bar{u}_j} - \sigma^2 \left[\frac{1}{2} \frac{\partial^2 \bar{u}_i \bar{u}_j}{\partial x_k \partial x_k} - \frac{\partial \bar{u}_i}{\partial x_k} \frac{\partial \bar{u}_j}{\partial x_k} \right] \\ & + \frac{\sigma^4}{2} \left[\frac{\partial^2}{\partial x_l \partial x_l} \left(\frac{1}{4} \frac{\partial^2 \bar{u}_i \bar{u}_j}{\partial x_k \partial x_k} - \frac{\partial \bar{u}_i}{\partial x_k} \frac{\partial \bar{u}_j}{\partial x_k} \right) + \frac{\partial^2 \bar{u}_i}{\partial x_k \partial x_l} \frac{\partial^2 \bar{u}_j}{\partial x_k \partial x_l} \right] + \mathcal{O}(\sigma^6). \end{aligned} \quad (3.8)$$

It is important to note that every single term in the approximations for the filtered advection term is an explicitly filtered term. This is crucial in order to ensure that the approximations of the filtered advection term decay as fast as the Gaussian filter kernel (times a real finite constant) in spectral space, which is shown in appendix A. The dyadic product of the filtered velocities used in classical LES, $\bar{u}_i \bar{u}_j$, for instance, decays slower than a Gaussian (times a real finite constant) in spectral space. As explained in section 2.3 for the more intuitive case of a filter kernel with compact support in spectral space, this can cause the violation of the definition of the filtered velocity if the model for τ_{ij} is not exact.

3.2. Correlation with the filtered advection term

The expressions for the filtered advection term derived in the previous section become formally more accurate by including successive terms of increasing order with respect to the filter width. In this section, the accuracy of the predictions of the filtered advection term are directly evaluated for different orders based on the explicitly filtered velocity field of HIT. The velocity field is obtained from DNS of forced HIT with a Taylor-scale Reynolds number of $\text{Re}_\tau = 75$. The simulations are carried out with a second order accurate finite-volume flow solver with 256^3 mesh cells. The exact same dataset has been used in several previous studies where more details on the flow physics and the numerical solution can be found (see, e.g., Hausmann *et al.* (2022, 2023a,b)).

The filtered advection term is abbreviated with

$$\mathcal{A}_{ij} = \overline{u_i u_j}, \quad (3.9)$$

and compared to different modeled filtered advection terms, $\mathcal{A}_{ij}^{\text{mod}}$, that are obtained by truncating the Taylor series expansion for the filtered advection term after terms proportional to the zeroth order in σ (equation (3.6)), after terms proportional to the second order in σ (equation (3.7)), and after terms proportional to the fourth order in σ (equation (3.8)), respectively.

Figure 2 shows the diagonal and figure 3 the off-diagonal components of the joint probability density functions (PDF) between $\mathcal{A}_{ij}^{\text{mod}}$ for different orders and \mathcal{A}_{ij} obtained from explicit filtering. The DNS is explicitly filtered with a Gaussian filter kernel with a filter width $\sigma/\Delta x_{\text{DNS}} = 4$, where Δx_{DNS} is the mesh spacing of the DNS. By including terms with increasing order in σ , the diagonal and off-diagonal components of $\mathcal{A}_{ij}^{\text{mod}}$ and \mathcal{A}_{ij} are increasingly correlated. For comparison, the joint PDF is also shown with the dyadic product of the filtered velocities, $\bar{u}_i \bar{u}_j$. Including terms up to the second order in σ is sufficient to predict a filtered advection term that possesses a significantly higher

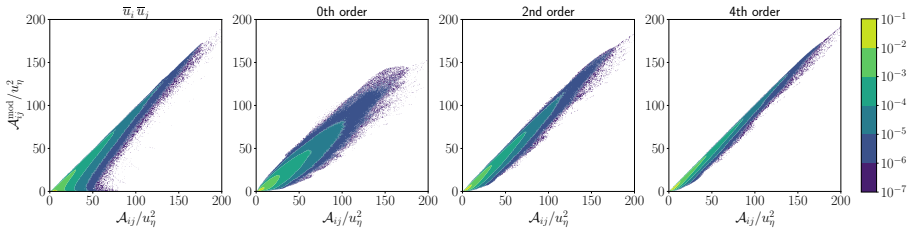


FIGURE 2. Joint PDF between the diagonal components ($i = j$) of different modeled filtered advection terms and the explicitly filtered advection term at a filter width of $\sigma/\Delta x_{\text{DNS}} = 4$.

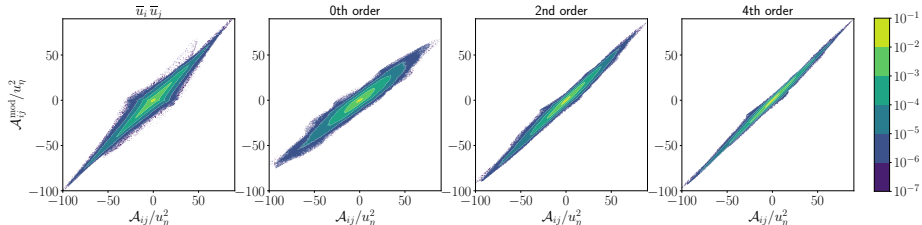


FIGURE 3. Joint PDF between the off-diagonal components ($i \neq j$) of different modeled filtered advection terms and the explicitly filtered advection term at a filter width of $\sigma/\Delta x_{\text{DNS}} = 4$.

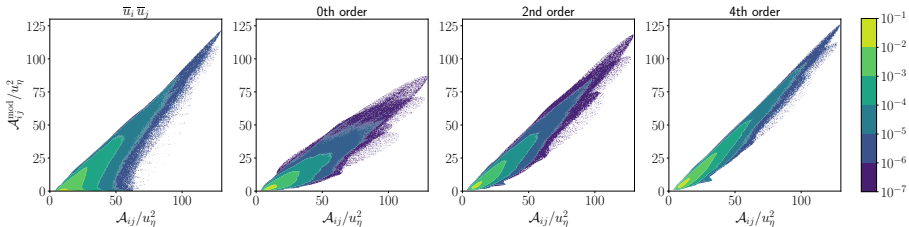


FIGURE 4. Joint PDF between the diagonal components ($i = j$) of different modeled filtered advection terms and the explicitly filtered advection term at a filter width of $\sigma/\Delta x_{\text{DNS}} = 8$.

correlation with the explicitly filtered advection term than the dyadic product of the filtered velocities. Similar joint PDFs are shown for a larger filter width of $\sigma/\Delta x_{\text{DNS}} = 8$ for the diagonal components in figure 4 and for the off-diagonal components in figure 5. Although the correlations between $\mathcal{A}_{ij}^{\text{mod}}$ and \mathcal{A}_{ij} are lower for the larger filter width, a similar increase of the correlation can be observed by including terms of increasing order in σ . Also for the filter width $\sigma/\Delta x_{\text{DNS}} = 8$, including terms up to σ^2 is sufficient to obtain a higher correlation than with the dyadic product of the filtered velocities.

The zeroth order term, which possesses a weaker correlation with the filtered advection term than the dyadic product of the filtered velocities, is used in existing models that approximate the filtered advection term (Lund 2003; Bose *et al.* 2010; Singh *et al.* 2012). It may be argued that in these models and in classical LES the advection term is not applied alone but in conjunction with a modeled τ_{ij} . However, in the vast majority of LES applications, the dyadic product of the filtered velocities, $\bar{u}_i \bar{u}_j$, is supplemented with a turbulent viscosity contribution, i.e., a term proportional to the strain-rate tensor, which is known to be poorly correlated with τ_{ij} (Liu *et al.* 1994; Borue & Orszag 1998; Horiuti 2003).

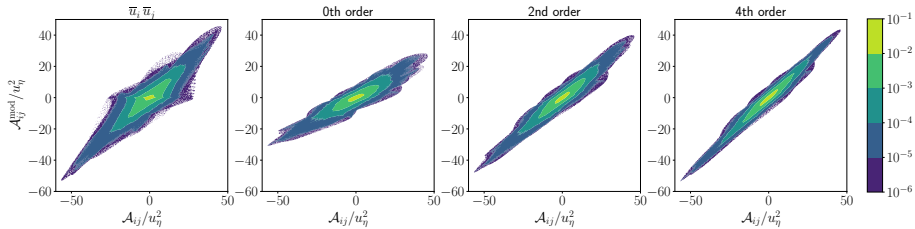


FIGURE 5. Joint PDF between the off-diagonal components ($i \neq j$) of different modeled filtered advection terms and the explicitly filtered advection term at a filter width of $\sigma/\Delta x_{\text{DNS}} = 8$.

3.3. Energy transfer

An expression for $\mathcal{A}_{ij}^{\text{mod}}$ that is highly correlated with \mathcal{A}_{ij} is not guaranteed to be a suitable LES closure model. A crucial property of a suitable closure model is the prediction of realistic energy transfer between the filtered and subfilter scales. The energy transfer resulting from the filtered advection term is denoted as T and defined as

$$T = -\overline{u_i} \frac{\partial}{\partial x_j} \mathcal{A}_{ij}. \quad (3.10)$$

The modeled energy transfer resulting from the modeled filtered advection term, $\mathcal{A}_{ij}^{\text{mod}}$, is denoted as T^{mod} .

On average, the filtered advection term removes energy from the filtered scales, distinguishing it from the dyadic product of the filtered velocities used in classical LES, $\overline{u_i u_j}$, which does not cause any net energy transfer between filtered and subfilter scales. The pointwise energy transfer of the filtered advection term, however, can be positive and negative, representing a bidirectional energy exchange between the scales.

Lund (2003) makes the correct observation that the approximation of the filtered advection term $\overline{u_i u_j}$ causes a nonzero net energy transfer and this net energy transfer is referred to as “false dissipation”. However, due to the fact that the filtered advection term, that $\overline{u_i u_j}$ is supposed to approximate, produces a nonzero net energy transfer, “false dissipation” is certainly not a suitable term. The energy transfer induced by $\overline{u_i u_j}$ may not be very accurate, but the fact that there is net energy transfer is a desirable property.

Figure 6 shows the PDF of the energy transfer in forced HIT of the FDNS together with the modeled advection up to terms of the zeroth, second, and fourth order for the filter widths $\sigma/\Delta x_{\text{DNS}} = 4$ and $\sigma/\Delta x_{\text{DNS}} = 8$. The PDF of the energy transfer is skewed and possesses a longer tail in the negative direction, which is associated to a removal of energy from the filtered scales. However, a significant portion of the energy transfer is positive. The positive energy transfer is caused by backscattering of energy from the subfilter scales to the filtered scales and by positive energy transfer between the filtered scales themselves. In figure 6 it can be observed that the positive energy transfer is captured very well by the modeled advection term up to the fourth order, even for the larger filter width. With increasing order of the modeled advection term, the PDFs of the energy transfer approach the correct PDF from the FDNS. However, for all orders of the modeled advection term, the events associated to significant removal of kinetic energy from the filtered scales occur too rarely.

The total energy transfer is further analyzed by examining the fraction of the energy transfer of the filtered advection term that is captured by the modeled filtered advection term for different filter widths and different order σ^n , as shown in figure 7. The total

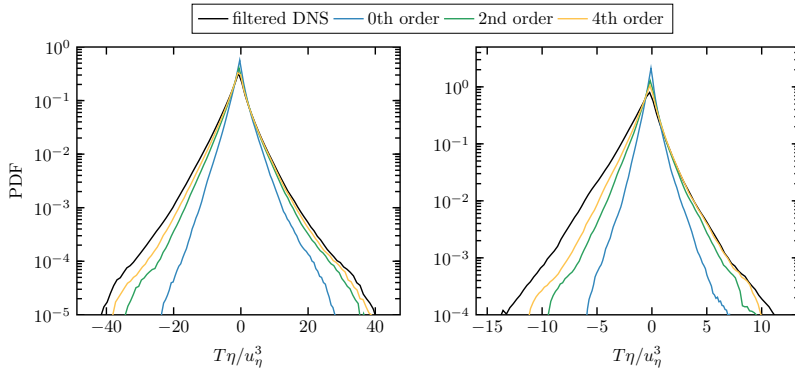


FIGURE 6. PDF of the energy transfer of the filtered advection term in forced HIT for the filter widths $\sigma/\Delta x_{\text{DNS}} = 4$ (left) and $\sigma/\Delta x_{\text{DNS}} = 8$ (right).

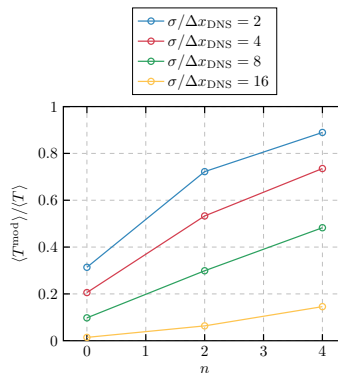


FIGURE 7. Fraction of the total energy transfer captured by the model for the filtered advection term for different orders n and different filter widths σ .

energy transfer is denoted as $\langle T \rangle$, where the angular brackets indicate ensemble averaging. It is observed that the total energy that is removed from the filtered scales is predicted increasingly accurately by including terms of increasing order n and decreasing filter width. Therefore, a sufficient removal of energy would require including terms of a high order n for large filter widths. Although it is straightforward to derive high order expressions for the filtered advection term, high orders in σ are associated to high order spatial derivatives of the filtered velocity, which can become expensive to evaluate and potentially less accurate if the filter width and mesh spacing are kept constant. Since the correlation of the modeled filtered advection term with the filtered advection term is still high for large filter widths, it can be beneficial in practice to supplement the model for the filtered advection term with a simple dissipative mechanism for large filter widths instead of increasing the order n .

In figure 8, the total energy transfer and its approximations are shown as a function of the filter width. In addition to the approximations of the filtered advection term with different orders, the energy transfer is also shown for a Smagorinsky type approximation that is given as

$$\mathcal{A}_{ij}^{\text{mod}} = -(C_S \sigma)^2 |\bar{S}| 2\bar{S}_{ij}, \quad (3.11)$$

where \bar{S}_{ij} is the filtered strain-rate tensor, C_S is the Smagorinsky constant that is assumed as $C_S = 0.2$ for the remainder of this article, and $|\bar{S}|$ is a norm of the filtered strain-rate

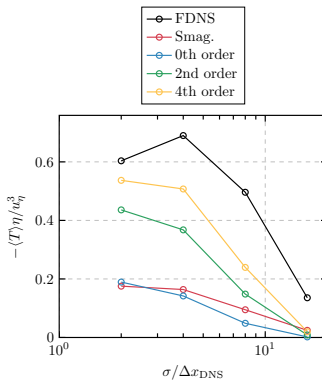


FIGURE 8. Total energy transfer for different approximations of the filtered advection term as a function of the filter width.

tensor that is defined as

$$|\bar{S}| = \sqrt{2\bar{S}_{ij}\bar{S}_{ij}}. \quad (3.12)$$

It is confirmed by examining their results presented in figure 8 that a higher order approximation of the filtered advection term significantly improves the predicted total energy transfer, but even for $n = 4$ some removal of energy from the filtered scales is missing. With the commonly used Smagorinsky approximation, an even larger discrepancy to the required energy transfer remains. Note that in classical LES where the advection term is the dyadic product of the filtered velocities $\bar{u}_i\bar{u}_j$, the Smagorinsky contribution is the only term of the approximation for the filtered advection term that leads to a nonzero net energy transfer.

According to Kolmogorov (1941), the flow statistics in the inertial range are independent of the viscosity, such that dimensional analysis suggests that $\langle T \rangle \propto \langle \epsilon \rangle$, where ϵ is the viscous dissipation of the unfiltered flow. Therefore, $\langle T \rangle$ does not depend on the filter width in the inertial range, which has been confirmed in HIT simulations of much larger Re_τ (see, e.g., Johnson (2022)). In the present HIT simulations the inertial range is associated with a filter width of approximately $\sigma/\Delta x_{DNS} \approx 4$, where the maximum of $-\langle T \rangle$ lies. Dimensional analysis also reveals that the energy transfer of the n th order approximation of the filtered advection term as well as the Smagorinsky approximation are constant in the inertial range. This suggests that supplementing the approximation of the filtered advection term, even with a very simple model such as the Smagorinsky model, can result in the correct energy transfer in the inertial range given that the constant C_S is chosen appropriately. A major advantage of combining the Smagorinsky model with the proposed approximation of the filtered advection term rather than combining it with the dyadic product of the filtered velocities is that a significant fraction of the energy transfer is already captured by the approximation of the filtered advection term.

If only the total energy transfer between filtered and subfilter scales is considered, supplementing the approximation for the filtered advection term with a Smagorinsky contribution appears to be a suitable intervention to obtain the correct energy transfer. However, to obtain a realistic filtered flow field, the energy must be removed from the correct scales, i.e., the spectral distribution of the energy transfer must be correct. The kinetic energy spectrum of the filtered velocity is altered by the energy transfer spectrum

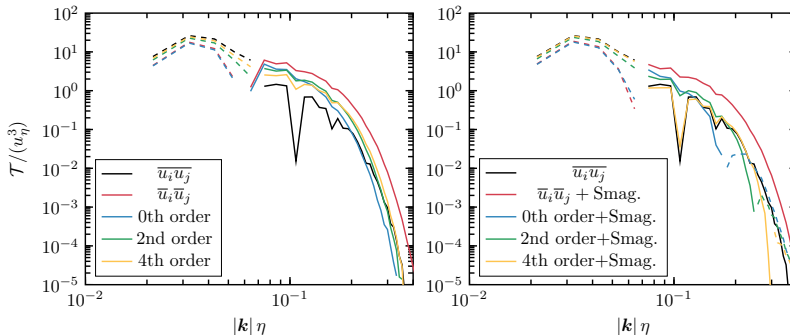


FIGURE 9. Energy transfer spectra for different approximations of the filtered advection term at a filter width of $\sigma/\Delta x_{\text{DNS}} = 4$. Dashed lines indicate negative energy transfer.

that is defined as

$$\mathcal{T}(k) = - \oint_{|\mathbf{k}|=k} \Re\{\hat{u}_i^*(\mathbf{k}) \widehat{\frac{\partial \mathcal{A}_{ij}}{\partial x_j}}(\mathbf{k})\} d\mathcal{S}(k), \quad (3.13)$$

where $\hat{\cdot}$ indicates the Fourier transform, \cdot^* indicates a complex conjugate, and \Re refers to the real part. The integration is carried out over spherical shells in wave number space $\mathcal{S}(k)$. According to Parseval's theorem

$$\langle T \rangle = \int_0^\infty \mathcal{T}(k) dk, \quad (3.14)$$

which means that \mathcal{T} integrates to zero for the dyadic product of the filtered velocities $\bar{u}_i \bar{u}_j$.

Figure 9 shows the energy transfer spectrum with the explicitly filtered advection term, with different orders of approximation of the filtered advection term, and with the dyadic product of the filtered velocities. Furthermore, the energy transfer spectra are shown with the approximations of the filtered advection term supplemented with the Smagorinsky term given in equation (3.11).

All of the energy transfer spectra are negative for the large filtered scales and positive for the small filtered scales, which means that all approximations transfer energy from the large to the small filtered scales. Since the net energy transfer of the dyadic product of the filtered velocities, $\bar{u}_i \bar{u}_j$, is zero, the small filtered scales receive exactly the same energy as is removed from the large filtered scales. With increasing order of the proposed approximations of the filtered advection term, the energy removed from the large filtered scales increases and the energy added to the small filtered scales decreases, such that with increasing order the energy transfer spectrum approaches that of the FDNS.

By adding the Smagorinsky term given in equation (3.11) to the approximations of the filtered advection term, a dissipative component is added. This additional dissipation is not sufficient for the dyadic product of the filtered velocities to predict an accurate energy transfer spectrum. The fourth order approximation of the filtered advection term together with the Smagorinsky term leads to a very accurate prediction of the energy transfer spectrum across the whole wave number range. Therefore, the Smagorinsky term not only provides the required total dissipation but also the correct spectral distribution, such that the energy transfer is correct at all wave numbers.

In summary, the fourth order approximation of the filtered advection term together with the Smagorinsky term can predict the correct total energy transfer and even the correct spectral distribution of the energy transfer. Furthermore, it is shown in the previous

sections that the fourth order approximation of the filtered advection term is highly correlated with the filtered advection term and that it does not introduce wave numbers in the filtered NSE that exceed the maximum wavenumber consistent with the definition of a filtered quantity.

3.4. Galilean invariance

In addition to producing accurate flow physics, the model for the filtered advection term must also comply with the fundamental principle that the observed physics is independent of the velocity of the observer, i.e., that Galilean invariance is satisfied. Galilean invariance is satisfied if the momentum equation in a frame of reference moving with the constant velocity \mathbf{u}_{ref} is the same as in the fixed frame of reference. If u_i is the velocity in the moving frame of reference, the velocity in the fixed frame is given as

$$\mathcal{U}_i = u_i(\mathbf{x} - \mathbf{u}_{\text{ref}}t, t) + u_{\text{ref},i}, \quad (3.15)$$

Since the filtered advection term $\overline{u_i u_j}$ can be verified to lead to a Galilean invariant filtered momentum equation, Galilean invariance of the modeled advection term is satisfied if

$$\overline{\mathcal{U}_i \mathcal{U}_j} - \mathcal{A}_{ij}^{\text{mod}}(\overline{\mathcal{U}_i}) = \overline{u_i u_j} - \mathcal{A}_{ij}^{\text{mod}}(\overline{u_i}). \quad (3.16)$$

that is, the modeled advection term produces the same additional terms when changing the frame of reference as the filtered advection term and the error introduced by modeling the filtered advection term is the same in all frames of reference.

The dyadic product of the filtered velocities turns out to exactly satisfy Galilean invariance since

$$\overline{\mathcal{U}_i \mathcal{U}_j} - \overline{\mathcal{U}_i} \overline{\mathcal{U}_j} = \overline{u_i u_j} - \overline{u_i} \overline{u_j}. \quad (3.17)$$

In practice, however, Galilean invariance is almost never satisfied because advection schemes with flux limiters and finite element stabilization terms typically introduce a velocity dependence of the discretization. In particular, this concerns implicit LES that inherently rely on the dissipative properties of the flux limiters or stabilization terms. Checking Galilean invariance of proposed approximations of the filtered advection term gives

$$\overline{\mathcal{U}_i \mathcal{U}_j} - \mathcal{A}_{ij}^{\text{mod}}(\overline{\mathcal{U}_i}) = \overline{u_i u_j} - \mathcal{A}_{ij}^{\text{mod}}(\overline{u_i}) + \underbrace{u_{\text{ref},i}(\overline{u_i} - \overline{\overline{u_i}})}_{\mathcal{O}(\sigma^2)} + \underbrace{(\overline{u_j} - \overline{\overline{u_j}})u_{\text{ref},j}}_{\mathcal{O}(\sigma^2)}, \quad (3.18)$$

for the zeroth order,

$$\begin{aligned} \overline{\mathcal{U}_i \mathcal{U}_j} - \mathcal{A}_{ij}^{\text{mod}}(\overline{\mathcal{U}_i}) &= \overline{u_i u_j} - \mathcal{A}_{ij}^{\text{mod}}(\overline{u_i}) \\ &+ u_{\text{ref},i} \underbrace{\left(\overline{u_j} - \overline{\overline{u_j}} + \frac{\sigma^2}{2} \frac{\partial^2 \overline{\overline{u_j}}}{\partial x_k \partial x_k} \right)}_{\mathcal{O}(\sigma^4)} + \underbrace{\left(\overline{u_i} - \overline{\overline{u_i}} + \frac{\sigma^2}{2} \frac{\partial^2 \overline{\overline{u_i}}}{\partial x_k \partial x_k} \right)}_{\mathcal{O}(\sigma^4)} u_{\text{ref},j}, \end{aligned} \quad (3.19)$$

for the second order, and

$$\begin{aligned}
\overline{u_i u_j} - \mathcal{A}_{ij}^{\text{mod}}(\overline{u_i}) &= \overline{u_i u_j} - \mathcal{A}_{ij}^{\text{mod}}(\overline{u_i}) \\
&+ u_{\text{ref},i} \underbrace{\left(\overline{u_j} - \overline{\overline{u_j}} + \frac{\sigma^2}{2} \frac{\partial^2 \overline{\overline{u_j}}}{\partial x_k \partial x_k} - \frac{\sigma^4}{4} \frac{\partial^4 \overline{\overline{u_j}}}{\partial x_l \partial x_l \partial x_k \partial x_k} \right)}_{\mathcal{O}(\sigma^6)} \\
&+ \underbrace{\left(\overline{u_i} - \overline{\overline{u_i}} + \frac{\sigma^2}{2} \frac{\partial^2 \overline{\overline{u_i}}}{\partial x_k \partial x_k} - \frac{\sigma^4}{4} \frac{\partial^4 \overline{\overline{u_i}}}{\partial x_l \partial x_l \partial x_k \partial x_k} \right)}_{\mathcal{O}(\sigma^6)} u_{\text{ref},j}, \quad (3.20)
\end{aligned}$$

for the fourth order. Since additional terms arise, Galilean invariance is not satisfied exactly. However, the third and fourth terms on the right-hand sides of equations (3.18)-(3.20) are small in the sense that they converge to zero for small filter widths with different orders. By comparing the terms with the Taylor series (3.2), it can be seen that they are of the same order in σ as the approximation for the filtered advection term. Therefore, as the order in σ increases, Galilean invariance is satisfied with increasing accuracy. This conclusion is not of a different quality than the violation of Galilean invariance of the commonly applied flux limiters and stabilization terms. The quantitative effect is studied in section 4.1.4.

4. A posteriori studies

4.1. Decaying turbulence

4.1.1. Simulation setup

As a first a posteriori test case, decaying turbulence in a fully periodic cubic domain is considered. The decay starts from the initially laminar and divergence-free velocity field

$$\mathbf{u} = U_0 \begin{pmatrix} \sin(2\pi y/L) \\ \sin(2\pi z/L) \\ \sin(2\pi x/L) \end{pmatrix}, \quad (4.1)$$

where L is the size of the cubic domain and U_0 the maximum velocity magnitude in each direction. The filtered initial velocity field with the filter width σ is therefore

$$\overline{\mathbf{u}} = U_0 \begin{pmatrix} \sin(2\pi y/L) \\ \sin(2\pi z/L) \\ \sin(2\pi x/L) \end{pmatrix} \exp(-(2\pi\sigma)^2/2L^2). \quad (4.2)$$

The Reynolds number can be defined as $\text{Re} = \rho_f U_0 L / \mu_f$. In the present study, the Reynolds number is chosen as $\text{Re} = 1000$. After a relatively short laminar initial phase, the flow field rapidly turns turbulent and decays until the initial kinetic energy is fully dissipated.

A DNS of the decaying turbulence is performed with a second order accurate finite volume solver that has been described and validated in many previous studies (Denner & van Wachem 2014; Bartholomew *et al.* 2018; Denner *et al.* 2020; Hausmann *et al.* 2022, 2024). The DNS are solved on a spatially uniform mesh with $N^3 = 256^3$ cells and a CFL-number of 0.1.

The LES are performed with the same finite volume solver as the DNS but with $N^3 = 64^3$ mesh cells and with a filter width $\sigma = \Delta x = L/N$, if not mentioned otherwise. The different LES differ in the representation of the filtered advection term and if the model for the filtered advection term is supplemented with a turbulent viscosity according to

the Smagorinsky model or not. The filtered advection term is approximated with the proposed second order or fourth order expression derived in section 3.1. For comparison, classical LES are performed that use either central differences or the van Leer flux limiter for the advection term. Details on the implementation of the central differences and the van Leer flux limiter in the present finite volume solver can be found in Denner & van Wachem (2015).

4.1.2. Results

In figure 10, the temporal evolution of different flow statistics is shown. In particular, figure 10 shows the kinetic energy of the filtered velocity

$$K = \frac{1}{2} \langle \bar{u}_i \bar{u}_i \rangle, \quad (4.3)$$

the viscous dissipation of the filtered velocity field

$$\epsilon = \mu_f \langle \frac{\partial \bar{u}_i}{\partial x_j} \frac{\partial \bar{u}_i}{\partial x_j} \rangle, \quad (4.4)$$

and the total removal of energy from the filtered scales that includes the energy transferred to the subfilter scales and that is given as $-dK/dt$. The kinetic energy of the filtered scales is normalized by its initial value $K(t=0)$ and the viscous dissipation and the total energy removal are normalized by the initial viscous dissipation $\epsilon(t=0)$. The time is normalized by a reference time $t_{\text{ref}} = L/U_0$.

The temporal evolution of the filtered kinetic energy predicted by the LES with the second and fourth order approximation of the filtered advection term closely resembles that of the FDNS. The classical LES with central differences and the Smagorinsky model decays too slow. Both observations are consistent with the a priori investigations of the energy transfer spectrum in section 3.3 that show that the dyadic product of the filtered velocities with the Smagorinsky model removes too little energy from the large filtered scales and transfers too much energy to the small filtered scales. Furthermore, it can be observed in figure 10 that the viscous dissipation of the filtered field is overpredicted by the classical LES with the Smagorinsky model. This seems to contradict the too slow energy decay of the classical LES. However, the viscous dissipation of the filtered field makes up only approximately 15% of the total energy removal at the present filter width. Therefore, the majority of the energy removal from the filtered scales is caused by the filtered advection term. The second and fourth order approximation of the filtered advection term predict the viscous dissipation of the filtered field and the total energy removal well, whereas including terms of higher order leads to improved results.

More insights can be obtained by considering the kinetic energy spectrum at different times of the decay as shown in figure 11. At all of the three time instants, the classical LES with the Smagorinsky model predicts too high energy at the high wave numbers, confirming the insufficient removal of energy. The approximations of the filtered advection term including terms up to second and fourth order predict a much more accurate spectrum, but the energy at the smallest filtered scales is slightly overestimated consistent with the a priori observation that only a part of the energy transfer is captured that increases with the order. It should be noted that the spectra at the small wave numbers are not statistically meaningful because single realizations are considered and only very few small wave number modes exist.

As suggested by the a priori analysis, supplementing the second and fourth order approximation of the filtered advection term with a turbulent viscosity according to the Smagorinsky model can give the right total energy transfer and even the right spectral

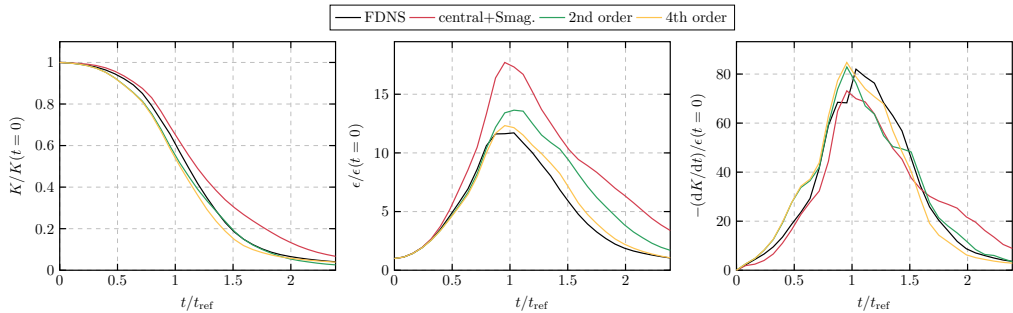


FIGURE 10. Temporal evolution of the filtered kinetic energy, viscous dissipation, and the total energy removal for the FDNS, the classical LES with central differences and the Smagorinsky model, and the LES with the second and fourth order approximation of the filtered advection term.

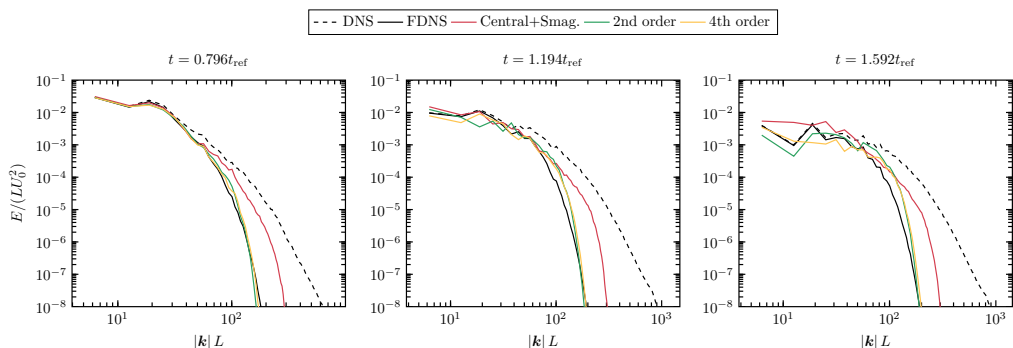


FIGURE 11. Kinetic energy spectrum at different times during the decay for the FDNS, the classical LES with central differences and the Smagorinsky model, and the LES with the second and fourth order approximation of the filtered advection term. The DNS spectrum is shown as reference.

distribution of the energy transfer. In figure 12 the same kinetic energy spectra are shown but the second and fourth order approximations of the filtered advection term are supplemented with the Smagorinsky model. With the additional turbulent viscosity, the LES with the second and fourth order approximation of the filtered advection term reproduce the kinetic energy spectrum of the FDNS accurately for all the three time instants.

A known property of classical LES with a turbulent viscosity model is that they fail to predict the correct topology of flow structures of the filtered velocity and, instead, predict a flow field that is topologically similar to a turbulent flow with a smaller Re (Kamal & Johnson 2024). This is confirmed in figure 13, where the absolute filtered velocity is depicted in a slice during the turbulent decay for the FDNS, the classical LES with the Smagorinsky model, and the fourth order approximation of the filtered advection with the Smagorinsky model. The classical LES produces very elongated flow structures whereas the topology of the explicitly filtered velocity is much more isotropic. With the fourth order approximation of the filtered advection term, the filtered velocity structures are similar in size and magnitude to the FDNS.

4.1.3. Behavior under mesh refinement

A fundamental property when solving for the filtered flow field is that the solution converges under mesh refinement, i.e., after a minimum resolution is ensured, further

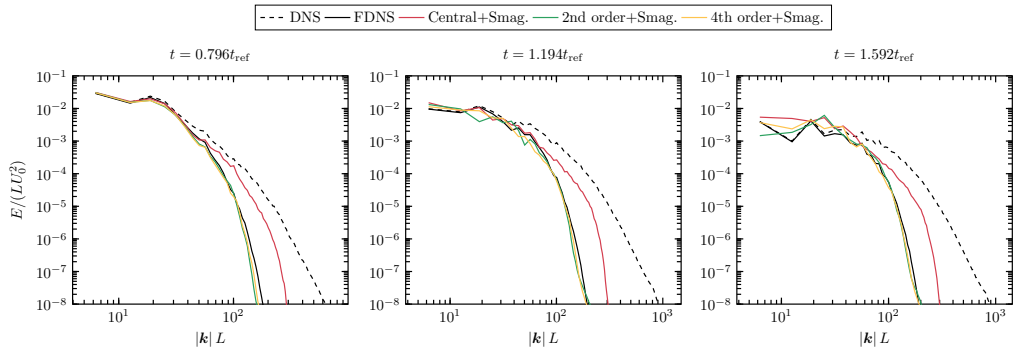


FIGURE 12. Kinetic energy spectrum at different times during the decay for the FDNS, the classical LES with central differences and the Smagorinsky model, and the LES with the second and fourth order approximation of the filtered advection term with the Smagorinsky model. The DNS spectrum is shown as reference.

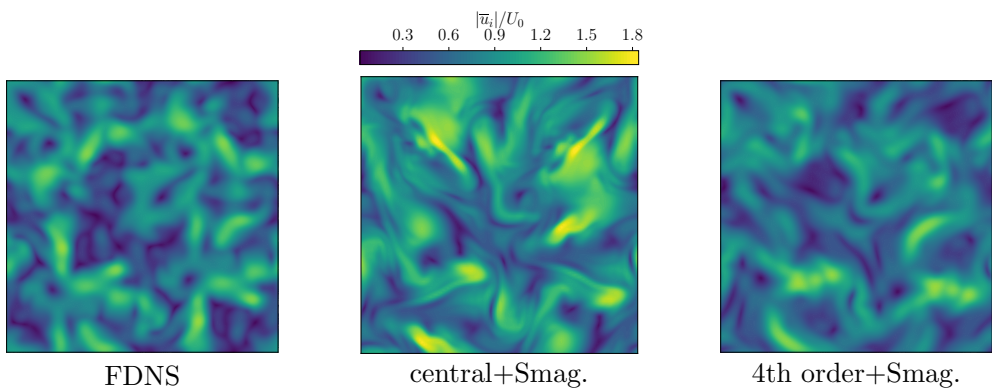


FIGURE 13. Slice of the absolute velocity during the decay at $t = 1.194t_{\text{ref}}$ for the FDNS, the classical LES with central differences and the Smagorinsky model, and the fourth order approximation of the filtered advection term with the Smagorinsky model.

refinement does not alter the statistics of the filtered flow field. Figure 14 shows the kinetic energy spectra at $t = 1.194t_{\text{ref}}$ of the LES with the fourth order approximation of the filtered advection term, the classical LES with the central differences and the Smagorinsky model, and the classical LES with the van Leer flux limiter and the Smagorinsky model with 64^3 , 96^3 , and 128^3 mesh cells. The kinetic energy spectrum with the fourth order approximation is essentially independent of the resolutions, which means that $\Delta x = \sigma$ is a sufficient resolution for the fourth order approximation. An even coarser resolution may be also sufficient, especially when adding an extra turbulent viscosity that further reduces the amplitudes associated to large wavenumbers and, therefore, the discretization error. With the classical LES and central differences, the kinetic energy spectrum possesses much larger wave numbers and the spectrum changes as the resolution is increased from 64^3 to 96^3 . Further refinement does not influence the spectrum because the turbulent viscosity from the Smagorinsky model dissipates the very small flow structures. The classical LES with the van Leer flux limiter behaves differently. The kinetic energy spectrum differs significantly from the spectrum obtained with central differences and no convergence is observed under the tested refinements. This shows that the statistics of classical LES can strongly depend on the advection scheme and the resolution.

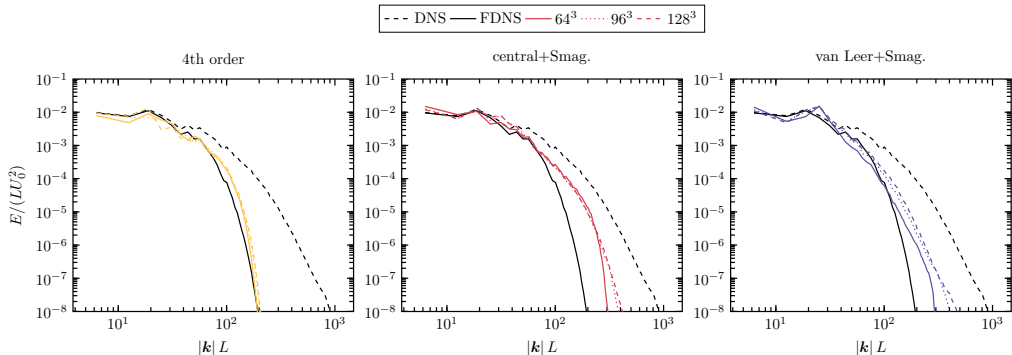


FIGURE 14. Kinetic energy spectrum at $t = 1.194t_{\text{ref}}$ and for different resolutions obtained with the fourth order approximation of the filtered advection term, the classical LES with the central differences and the Smagorinsky model, and the classical LES with the van Leer flux limiter and the Smagorinsky model.

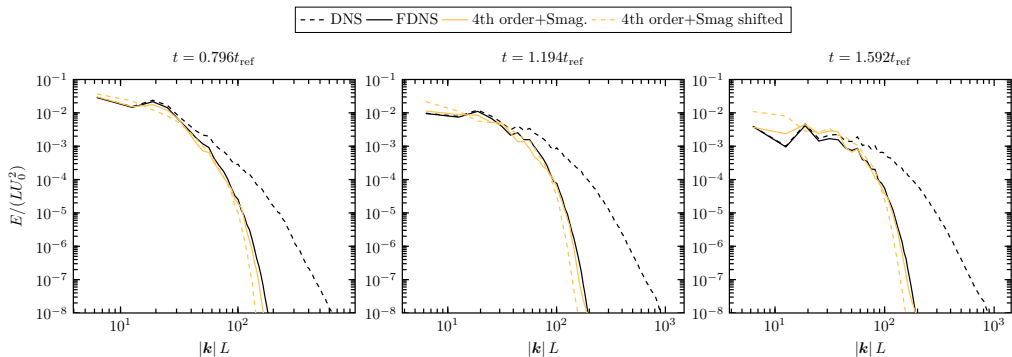


FIGURE 15. Kinetic energy spectrum at different times during the decay for the FDNS and the LES with the 4th order approximation of the filtered advection term with a turbulent viscosity according to the Smagorinsky model performed in different frames of reference.

4.1.4. Galilean invariance

A potential drawback of the proposed approximation of the filtered advection term is that it is not exactly Galilean invariant but only Galilean invariant up to the order of accuracy of the approximation. To assess the practical implications, the LES of the fourth order approximation with the Smagorinsky model are repeated in a frame of reference shifted by $10U_0$, i.e., by ten times the amplitude of the initial velocity field. An exactly Galilean invariant model should predict the identical statistics after the results are transformed back into the original frame, which is the case for the central differences but not for the van Leer flux limiter or other common flux limiters. Figure 15 shows the kinetic energy spectra of the results in the shifted frame of reference after transformation back into the original frame compared to the spectra obtained with the LES in the original frame. It is observed that the spectra are indeed not identical, but the differences are minor and of the order of the uncertainty of the approximation itself. Since even a significant change of the frame of reference causes only a minor change in the turbulence statistics, the approximate fulfillment of Galilean invariance does not seem to be of practical relevance for most of the cases.

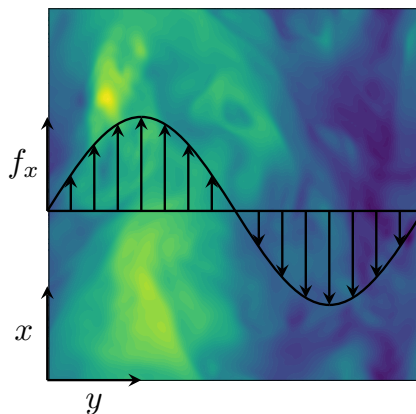


FIGURE 16. Illustration of the turbulent shear flow configuration that is driven by a momentum source f_x in the x-direction varying with the shape of a sine in the y-direction.

4.2. Turbulent shear flow

4.2.1. Simulation setup

A statistically inhomogeneous and anisotropic turbulent shear flow is considered as second test case to evaluate the proposed approximations for the filtered advection term. The same turbulent shear flow has been investigated in previous studies (Hausmann *et al.* 2022, 2023b) and is briefly summarized in the following.

The turbulent shear flow is solved in a fully periodic cube with the side length L and it is driven by a sine-shaped momentum source \mathbf{f} , as illustrated in figure 16. Mathematically, the momentum source driving the shear flow is given as

$$\mathbf{f}(y) = f_{\max} \sin(2\pi y/L) \mathbf{e}_x, \quad (4.5)$$

where f_{\max} is the amplitude of the momentum source and \mathbf{e}_x is the unit vector in the x-direction. With these quantities, a velocity scale u_{shear} and a corresponding Reynolds number $\text{Re}_{\text{shear}} = \rho_f u_{\text{shear}} L / \mu_f$ can be defined that is $\text{Re}_{\text{shear}} = 3115$ in the present case. The DNS, which is described in more detail in Hausmann *et al.* (2022), is carried out with the same finite volume solver that is used for the decaying turbulence on a uniform mesh with $N^3 = 128^3$ cells.

LES are performed on coarser meshes with $N^3 = 32^3$ and $N^3 = 16^3$ cells and are driven by the filtered momentum source

$$\bar{\mathbf{f}}(y) = f_{\max} \sin(2\pi y/L) \exp(-(2\pi\sigma)^2/2L^2) \mathbf{e}_x. \quad (4.6)$$

4.2.2. Results

Figure 17 shows the mean of the filtered velocity and the mean correlations of the fluctuations of the filtered velocity for the different LES, where a fluctuation of a flow quantity Φ is indicated as $\Phi' = \Phi - \langle \Phi \rangle$. With the finer resolution and the small filter width $\sigma = \Delta x = L/32$, the classical LES with central differences and the LES with the fourth order approximation of the filtered advection term, both with the Smagorinsky model, predict the mean filtered velocity profile very accurately. However, differences are observed in the filtered velocity correlations. The classical LES with central differences predicts a too large magnitude of $\langle \bar{u}'\bar{v}' \rangle$ and significantly overpredicts $\langle \bar{u}'\bar{u}' \rangle$, whereas

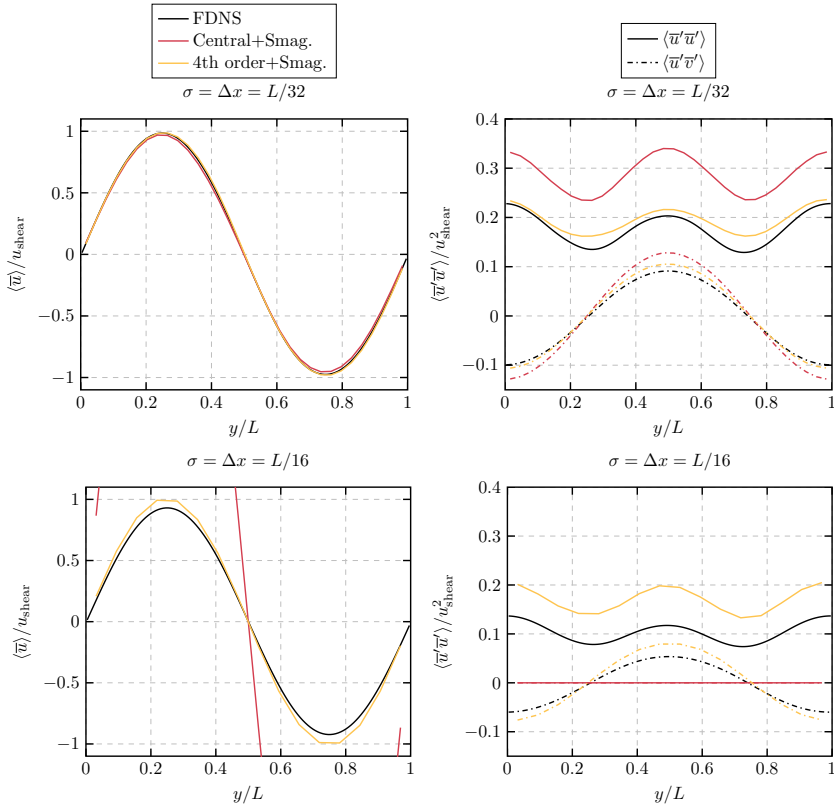


FIGURE 17. Filtered mean velocity and correlations of the filtered velocity fluctuations for two different filter widths of the turbulent shear flow configuration. The results of the classical LES with central differences and LES with the fourth order series expansion are shown, both with the Smagorinsky model.

the fourth order approximation of the advection term leads to accurate predictions of the correlations. The significant overprediction of the streamwise correlations by classical LES is a well-known phenomenon from wall-bounded flows that can be, at least partially, attributed to the inconsistent treatment of wall-boundary conditions in coarse LES (see, e.g., Bae *et al.* (2018)). The fact that $\langle \bar{u}' \bar{u}' \rangle$ is overestimated by classical LES in an unconfined turbulent shear flow suggests that the misalignment of the dyadic product of the filtered velocities with the filtered advection term also plays a role. With the fourth order approximation that is shown to be highly correlated with the filtered advection term, $\langle \bar{u}' \bar{u}' \rangle$ is predicted well.

Figure 17 also shows the results for coarser LES with $\sigma = \Delta x = L/16$. With such a coarse resolution, the classical LES does not turn turbulent and even relaminarizes when being initialized from a turbulent field which is why it leads to a very large mean velocity and zero fluctuations. The explicitly filtered mean velocity differs only slightly from the filtered mean velocity with $\sigma = \Delta x = L/32$ and is predicted accurately with the LES using the fourth order approximation of the filtered advection term. The correlations of the filtered velocity fluctuations change drastically with the increasing filter width, which is captured to some extent by the LES with the fourth order approximation of the filtered advection term.

5. Guidelines for implementation

Although the approximation for the filtered advection term including terms up to the fourth order, as given in equation (3.8), is a relatively long expression, its implementation is conceptually simple. It is very common that flow solvers that rely on the dyadic product of the filtered velocities as advection term treat the advection term at least partially implicit. Typically, iterations are carried out during which the non-linear advection term is updated with filtered velocities from the previous iteration until a norm of the difference of the predicted filtered velocities between two consecutive iterations is below a threshold. When the proposed approximation of the filtered advection term is implemented, the implementation of the classical advection term (dyadic product of the filtered velocities) is replaced with a discretized form of equation (3.6), (3.7), or (3.8), depending on the desired order. The structure of the iterations over the non-linear term depends on the specific flow solver but in general one iteration can be summarized as follows:

(i) Compute the approximation of $u_i u_j$ (without the filtering operation) from the filtered velocity of the previous iteration up to the desired order given in equations (3.6)-(3.8).

(ii) Perform the explicit filtering operation with a Gaussian filter kernel to obtain an approximation of $\overline{u_i u_j}$ from the previously computed approximation of $u_i u_j$.

(iii) Solve the filtered NSE with the approximation for $\overline{u_i u_j}$ as the advection term to obtain the predicted filtered velocity of the present iteration.

(iv) Compute a norm of the difference between the predicted velocity of the present iteration and the predicted velocity of the previous iteration.

(v) If the norm exceeds the convergence threshold, start another iteration. Otherwise, start with the next time step.

This solution algorithm turns out to be numerically very robust. For instance, even when repeating the simulations of the decaying turbulence configuration with the fourth order approximation of the filtered advection term as discussed in section 4.1 but with zero viscosity (infinite Reynolds number) and a CFL-number of one, a stable numerical solution is obtained requiring not more than three to four iterations per time step.

6. Conclusions

This article addresses the widely overlooked conceptual inconsistency of classical LES that the commonly used advection term, $\overline{u_i u_j}$, introduces higher wave numbers in the filtered NSE than consistent with the definition of a filtered equation. Consequently, the filtered velocity gets contaminated with high wave number content and numerical interventions are required, such as flux limiters, stabilization terms, or dealiasing, to capture the solution with coarse numerical resolution. Alternatively, the filtered advection term is modeled directly in the present article with an expression that contains only filtered terms and, therefore, leads to consistent filtered NSE. An exact expression is derived that is an infinite series expansion in powers of the filter width. As shown in a priori studies of HIT, retaining only a few terms of the series expansion leads to a model that is strongly correlated with the filtered advection term. A posteriori studies of decaying turbulence and a turbulent shear flow demonstrate that the proposed approximation of the filtered advection term is stable without any additional numerical interventions and that it predicts realistic filtered flow structures and filtered velocity correlations. Furthermore, it is shown that the predicted energy spectrum converges under mesh refinement and that Galilean invariance is satisfied in good approximation in

practice. The consistent and accurate approximation of the filtered advection proposed in the present article is a step towards more reliable and interpretable LES.

Funding. This research was funded by the Deutsche Forschungsgemeinschaft (DFG, German Research Foundation): —Project-ID 457509672.

Declaration of interests. The authors report no conflict of interest.

Data availability statement. The data that support the findings of this article are openly available in the repository <https://doi.org/10.5281/zenodo.18999736>.

Author ORCIDs.

Max Hausmann: <https://orcid.org/0000-0002-4342-4749>.

Berend van Wachem: <https://orcid.org/0000-0002-5399-4075>.

Appendix A. Spectral decay of the filtered advection term

Assuming that the velocity is bounded for all wave numbers, i.e., there exists a real finite constant C_u such that

$$|\hat{u}_i(\mathbf{k})| < C_u, \quad \forall \mathbf{k} \in \mathbb{R}^3, \quad (\text{A } 1)$$

where $\hat{\cdot}$ indicates the Fourier transform, the filtered advection term $\overline{u_i u_j}$ decays as rapidly as a Gaussian in spectral space

$$\lim_{|\mathbf{k}| \rightarrow \infty} |\hat{G}(\mathbf{k}) \widehat{\overline{u_i u_j}}(\mathbf{k})| < \lim_{|\mathbf{k}| \rightarrow \infty} |C_G \hat{G}(\mathbf{k})|, \quad (\text{A } 2)$$

for a finite real constant C_G .

In the following it is shown that the proposed approximation of $\overline{u_i u_j}$, which contains terms of the type

$$\frac{\partial^n \overline{u_i u_j}}{\partial (\sigma^2)^n},$$

also decays at least as rapidly as a Gaussian with standard deviation σ .

After applying the convolution theorem, the Fourier transform of the terms in the series expansion can be written as

$$\widehat{\frac{\partial^n}{\partial (\sigma^2)^n} (\overline{u_i u_j})}(\mathbf{k}) = \hat{G}(\mathbf{k}) \frac{\partial^n}{\partial (\sigma^2)^n} \widehat{\overline{u_i u_j}}(\mathbf{k}). \quad (\text{A } 3)$$

Differentiating the Fourier transform of a Gaussian with respect to σ^2 gives

$$\frac{\partial \hat{G}(\mathbf{k})}{\partial (\sigma^2)} = -\frac{|\mathbf{k}|^2}{2} \hat{G}(\mathbf{k}), \quad (\text{A } 4)$$

such that the n th derivative of the Fourier transform of the dyadic product is given as

$$\begin{aligned} \frac{\partial^n}{\partial (\sigma^2)^n} \widehat{\overline{u_i u_j}}(\mathbf{k}) &= \frac{\partial^n}{\partial (\sigma^2)^n} \int_{\mathbb{R}^3} \hat{G}(\mathbf{p}) \hat{G}(\mathbf{k} - \mathbf{p}) \hat{u}_i(\mathbf{p}) \hat{u}_j(\mathbf{k} - \mathbf{p}) \, \mathrm{d}\mathbf{p} \\ &= \int_{\mathbb{R}^3} P(|\mathbf{p}|^2, |\mathbf{k} - \mathbf{p}|^2) \hat{G}(\mathbf{p}) \hat{G}(\mathbf{k} - \mathbf{p}) \hat{u}_i(\mathbf{p}) \hat{u}_j(\mathbf{k} - \mathbf{p}) \, \mathrm{d}\mathbf{p}, \end{aligned} \quad (\text{A } 5)$$

where P is a polynomial. Since the velocity is bounded, there exists a real finite constant C_{ij} that satisfies

$$\lim_{|\mathbf{k}| \rightarrow \infty} \left| \frac{\widehat{\partial^n (\bar{u}_i \bar{u}_j)}(\mathbf{k})}{\partial(\sigma^2)^n} \right| < \lim_{|\mathbf{k}| \rightarrow \infty} \left| C_{ij} \hat{G}(\mathbf{k}) \int_{\mathbb{R}^3} |P| \hat{G}(\mathbf{p}) \hat{G}(\mathbf{k} - \mathbf{p}) \hat{u}_i(\mathbf{p}) \hat{u}_j(\mathbf{k} - \mathbf{p}) \mathrm{d}\mathbf{p} \right|. \quad (\text{A } 6)$$

Since a Gaussian decays faster than any polynomial can grow,

$$\int_{\mathbb{R}^3} |P| \hat{G}(\mathbf{p}) \hat{G}(\mathbf{k} - \mathbf{p}) \hat{u}_i(\mathbf{p}) \hat{u}_j(\mathbf{k} - \mathbf{p}) \mathrm{d}\mathbf{p}$$

is bounded and there exists a real finite constant C_G such that

$$\lim_{|\mathbf{k}| \rightarrow \infty} \left| \frac{\widehat{\partial^n (\bar{u}_i \bar{u}_j)}(\mathbf{k})}{\partial(\sigma^2)^n} \right| < \lim_{|\mathbf{k}| \rightarrow \infty} |C_G \hat{G}(\mathbf{k})|. \quad (\text{A } 7)$$

REFERENCES

- ARUN, R., KAMAL, M., COLONIUS, T. & JOHNSON, P. L. 2025 Normality-based analysis of multiscale velocity gradients and energy transfer in direct and large-eddy simulations of isotropic turbulence. *Journal of Fluid Mechanics* **1021**, A47.
- BAE, H. J., LOZANO-DURÁN, A., BOSE, S. T. & MOIN, P. 2018 Turbulence intensities in large-eddy simulation of wall-bounded flows. *Physical Review Fluids* **3** (1), 014610.
- BARTHOLOMEW, P., DENNER, F., ABDOL-AZIS, M., MARQUIS, A. & VAN WACHEM, B. 2018 Unified formulation of the momentum-weighted interpolation for collocated variable arrangements. *Journal of Computational Physics* **375**, 177–208.
- BORUE, V. & ORSZAG, S. A. 1998 Local energy flux and subgrid-scale statistics in three-dimensional turbulence. *Journal of Fluid Mechanics* **366**, 1–31.
- BOSE, S. T., MOIN, P. & YOU, D. 2010 Grid-independent large-eddy simulation using explicit filtering. *Physics of Fluids* **22** (10), 105103.
- DEARDORFF, J. W. 1970 A numerical study of three-dimensional turbulent channel flow at large Reynolds numbers. *Journal of Fluid Mechanics* **41** (02), 453.
- DENNER, F., EVRARD, F. & VAN WACHEM, B. 2020 Conservative finite-volume framework and pressure-based algorithm for flows of incompressible, ideal-gas and real-gas fluids at all speeds. *Journal of Computational Physics* **409**, 109348.
- DENNER, F. & VAN WACHEM, B. 2014 Numerical methods for interfacial flows with high density ratios and high surface tension. In *7th Conference of the International Marangoni Association*, , vol. 218. 23-26 June 2014, Vienna, Austria.
- DENNER, F. & VAN WACHEM, B. 2015 Numerical time-step restrictions as a result of capillary waves. *Journal of Computational Physics* **285**, 24–40.
- GERMANO, M. 1986 Differential filters of elliptic type. *The Physics of Fluids* **29** (6), 1757–1758.
- GERMANO, M., PIOMELLI, U., MOIN, P. & CABOT, W. H. 1991 A dynamic subgrid-scale eddy viscosity model. *Physics of Fluids A* **3** (7), 1760–1765.
- GHOSAL, S. 1996 An Analysis of Numerical Errors in Large-Eddy Simulations of Turbulence. *Journal of Computational Physics* **125** (1), 187–206.
- GRINSTEIN, F. F., MARGOLIN, L. G. & RIDER, W. J., ed. 2007 *Implicit Large Eddy Simulation: Computing Turbulent Fluid Dynamics*, 1st edn. Cambridge University Press.
- HAUSMANN, M., ELMESTIKAWY, H. & VAN WACHEM, B. 2024 Physically consistent immersed boundary method: A framework for predicting hydrodynamic forces on particles with coarse meshes. *Journal of Computational Physics* **519**, 113448.
- HAUSMANN, M., EVRARD, F. & VAN WACHEM, B. 2022 An efficient model for subgrid-scale velocity enrichment for large-eddy simulations of turbulent flows. *Physics of Fluids* **34** (11), 115135.

- HAUSMANN, M., EVRARD, F. & VAN WACHEM, B. 2023a Large eddy simulation model for two-way coupled particle-laden turbulent flows. *Physical Review Fluids* **8** (8), 084301.
- HAUSMANN, M., EVRARD, F. & VAN WACHEM, B. 2023b Wavelet-based modeling of subgrid scales in large-eddy simulation of particle-laden turbulent flows. *Physical Review Fluids* **8** (10), 104604.
- HORIUTI, K. 2003 Roles of non-aligned eigenvectors of strain-rate and subgrid-scale stress tensors in turbulence generation. *Journal of Fluid Mechanics* **491**, 65–100.
- JOHNSON, P. L. 2020 Energy Transfer from Large to Small Scales in Turbulence by Multiscale Nonlinear Strain and Vorticity Interactions. *Physical Review Letters* **124** (10), 104501.
- JOHNSON, P. L. 2022 A physics-inspired alternative to spatial filtering for large-eddy simulations of turbulent flows. *Journal of Fluid Mechanics* **934**, A30.
- KAMAL, M. & JOHNSON, P. L. 2024 Artificial bottleneck effect in large eddy simulations. *Physical Review Fluids* **9** (8), 084605.
- KOLMOGOROV, A. N. 1941 The local structure of turbulence in incompressible viscous fluid for very large Reynolds numbers. *Doklady Akademii Nauk Sssr* **30** (1890), 301–305.
- LEONARD, A. 1975 Energy Cascade in Large-Eddy Simulations of Turbulent Fluid Flows. In *Advances in Geophysics*, , vol. 18, pp. 237–248. Elsevier.
- LEONARD, A. 1997 Large-eddy simulation of chaotic convection and beyond. In *35th Aerospace Sciences Meeting and Exhibit*.
- LILLY, D. K. 1966 The representation of small scale turbulence in numerical simulation experiments. In *In: Proceedings of the IBM Scientific Computing Symposium on Environmental Sciences. Yorktown, NY, USA. National Center for Atmospheric Research (USA), NCAR Manuscript; No. 281.*, pp. 195–210.
- LILLY, D. K. 1992 A proposed modification of the Germano subgrid scale closure method. *Physics of Fluids A* **4** (3), 633–635.
- LIU, S., MENEVEAU, C. & KATZ, J. 1994 On the properties of similarity subgrid-scale models as deduced from measurements in a turbulent jet. *Journal of Fluid Mechanics* **275**, 83–119.
- LUND, T. 2003 The use of explicit filters in large eddy simulation. *Computers & Mathematics with Applications* **46** (4), 603–616.
- MARGOLIN, L. G., RIDER, W. J. & GRINSTEIN, F. F. 2006 Modeling turbulent flow with implicit LES. *Journal of Turbulence* **7**, N15.
- NICOUD, F. & DUCROS, F. 1999 Subgrid-scale stress modelling based on the square of the velocity gradient tensor. *Flow, Turbulence and Combustion* **62** (3), 183–200.
- SAGAUT, P. 2005 *Large Eddy Simulation for Incompressible Flows*, 3rd edn. Springer.
- SINGH, S., YOU, D. & BOSE, S. T. 2012 Large-eddy simulation of turbulent channel flow using explicit filtering and dynamic mixed models. *Physics of Fluids* **24** (8), 085105.
- SMAGORINSKY, J. 1963 General circulation experiments with the primitive equations. I: The basic experiment. *Month. Weath. Rev.* **91** (3), 99–165.
- STEIN, E. M. 2003 *Fourier Analysis: An Introduction*, 1st edn. New Jersey: Princeton University Press.
- STOLZ, S. & ADAMS, N. A. 1999 An approximate deconvolution procedure for large-eddy simulation. *Physics of Fluids* **11** (7), 1699–1701.
- STOLZ, S., ADAMS, N. A. & KLEISER, L. 2001 An approximate deconvolution model for large-eddy simulation with application to incompressible wall-bounded flows. *Physics of Fluids* **13** (4), 997.
- VREMAN, A. W. 2004 An eddy-viscosity subgrid-scale model for turbulent shear flow: Algebraic theory and applications. *Physics of fluids* **16** (10), 3670–3681.
- VREMAN, B., GEURTS, B. & KUERTEN, H. 1996 Large-eddy simulation of the temporal mixing layer using the Clark model. *Theoretical and Computational Fluid Dynamics* **8** (4), 309–324.